Electron tunneling rates between an atom and a corrugated surface

M. Taylor and P. Nordlander*
Department of Physics and Rice Quantum Institute, Rice University, Houston, Texas 77251
(Received 27 April 2001; published 30 August 2001)

An investigation of the lateral variations of the widths of atomic levels outside realistic surfaces is presented. The surfaces are modeled using finite clusters. The widths of the atomic levels are obtained by calculating the electronic structure of the atom/surface system and projecting the density of states upon the atomic levels. An investigation of cluster size dependence of the calculated widths is presented. It is shown that in the region near the surface, the widths are well converged already for relatively small clusters. An application to Li outside Al(001) and Si(110) surfaces shows that the lateral variation of the width of the Li(2s) level can be very significant.

DOI: 10.1103/PhysRevB.64.115422 PACS number(s): 73.90.+f, 79.20.Rf

I. INTRODUCTION

The shifts and broadening of atomic levels outside surfaces are important quantities determining the charge transfer probabilities in atom-surface scattering experiments.[1–3] The conventional models for the calculation of the widths of atomic resonances outside surfaces treat the substrate within a jellium model, with charge density varying only in the surface normal direction.[4–8] While these methods accurately predict the variation of the atom-surface electron tunneling rates with atom-surface separation, they cannot describe the lateral corrugation of the tunneling rate expected in the regions near the surface. In experiments involving low velocity atoms scattered against metal surfaces, the charge transfer often occur at sufficiently large distances from the surface that jellium models of the surface can be used.[9,10] For projectile energies larger than 1 keV and large incident angles, the charge transfer can occur close to the surface and in the region where lateral corrugation effects will be important. In several recent experiments involving the neutralization of noble gas ions with kinetic energies above 1 keV, clear evidence for a strong lateral corrugation of the electron tunneling rates have been presented.[11–13]

The extension of the conventional methods for the calculation of energy shift and broadening of atomic resonances to realistic corrugated surfaces represents a formidable task. A few applications have been made to study the influence of a weak corrugation and the effects of localized impurities and surface defects on the broadening and shift of atomic levels near surfaces.[14–16] The major obstacle preventing the application of these approaches to realistic corrugated surfaces is the difficulty in constructing the electron potential. The electron potential which is responsible for the tunneling barrier between the atom and the surface depend on the interaction between the atom and the surfaces. This potential must be calculated self-consistently rather than estimated by adding substrate and adsorbate potentials and simple image potentials describing the interaction between the adsorbate and the surface.

For small atom-surface distances, tight-binding methods have been applied to the calculation of the shift and broadening of the adsorbate levels.[17–19] In these approaches, the energy shift and broadening of the atomic levels are obtained by investigating the density of states of the atom/substrate system projected on the atomic levels. While the tight-binding models can account for the corrugated surface structure, they cannot be applied when the adsorbate is much more than one lattice space from the surface. Furthermore, since tight binding methods fail to describe the changes in the one-electron potential of the surface caused by the substantial charge rearrangements involved in chemisorption systems, neither the shifts nor the broadening of the adsorbate levels can be calculated quantitatively at small adsorbate-surface separations. Also, the dependence on semiempirical tight-binding parameters reduces the generality of these methods.

The present work builds on the previous tight-binding approaches[17–19] but is based on the self-consistent density functional formalism which provides a parameter free model of the electronic structure of the system and includes both exchange and correlation effects. The surface is modeled as a finite cluster, and the adsorbate-cluster electronic structure is resolved using general-purpose quantum chemistry codes. As these codes are equipped to study an arbitrary arrangement of atoms from first principles, the accessible range of adsorbate positions and surface structures is limited only by computational resources. No modification of the codes or the method is required when approaching a new system.

In Sec. II, the theoretical approach is presented. A method for the extraction of the width from the projected density of states is presented. In Sec. III, an investigation of cluster size effects is presented. In Sec. IV, results for the lateral variation of widths of the Li$(2s)$ level on Al(001) and Si(110) are presented. The conclusions are presented in Sec. V.

II. THEORY

For an atomic level of energy $\epsilon_{l\sigma}$ interacting with an infinite sea of conduction electrons, the spectral function takes the form

$$A_{l\sigma}(\omega)=\frac{1}{2\pi}\frac{\mathrm{Im}\,\Sigma_{l\sigma}}{(\omega-\epsilon_{l\sigma}-\mathrm{Re}\,\Sigma_{l\sigma})^2+(\mathrm{Im}\,\Sigma_{l\sigma})^2}, \qquad (1)$$

where $\Sigma_{l\sigma}$ is the energy dependent complex selfenergy of the atomic level. In the one-electron approximation, for a sub-

strate with large band width and weakly energy dependent density of states, the shift of the atomic level $\mathrm{Re}\,\Sigma$ is small and its broadening $\mathrm{Im}\,\Sigma_{l\sigma}$ is only weakly energy dependent. The spectral function is a Lorentzian with a half width $\Gamma = \mathrm{Im}\,\Sigma_{l\sigma}(\epsilon_{l\sigma})$. The spectral function of the level is equal to the density of states of the interacting system projected onto the atomic level. We will refer to the adsorbate-resolved energy spectrum as the projected density of states (JDOS). The broadening of the atomic resonance represents their transfer into the surface by tunneling,[17] so that the width of the spectral broadening is directly related to the tunneling rate. A property of the Lorentz distribution is that Γ is exactly the full width at half-maximum (FWHM), a quantity that is easily extracted from numerical results. Both Klamroth *et al.*[18] and Merino *et al.*[17] take advantage of this relation to calculate widths of atomic level outside corrugated surfaces by a numerical estimation of the FWHM.

The present work makes a similar attempt, but with a key difference; unlike these previous efforts, we cannot express the JDOS as an analytic function. The spectrum obtained from the cluster calculation consists of discrete, delta function peaks. From each electronic structure calculation, the projected density of states can be extracted and take the form

$$A_l(\epsilon) = \sum_k |C_{lk}|^2 \delta(\epsilon - \epsilon_k). \tag{2}$$

In this expression, A_l is the JDOS or spectral function, ϵ_k are the eigenvalues and C_{lk} are the corresponding eigenvector coefficients for the adsorbate level *l*. Note that both occupied and unoccupied eigenstates contribute to the JDOS.

The JDOS for a discrete system, such as a cluster, consists of individual delta function ''spikes'' rather than a smooth spectrum. To extract Γ, we must first transform the JDOS into a continuous function with a single recognizable peak. To make this transformation, we apply a Lorentzian broadening of width β to the calculated JDOS Eq. (2)

$$A_l'(\epsilon) = \sum_k |C_{lk}|^2 \frac{\beta/2\pi}{(\epsilon - \epsilon_k)^2 + (\beta/2)^2}. \tag{3}$$

When the energy level spacing is much less than Γ, the resonance width can be unambiguously determined by minimally broadening the JDOS and measuring its FWHM. Unfortunately, the range of interest for Γ corresponds to such closely spaced energy levels that extremely large clusters would be required. For example, if $\Gamma \approx 0.05$ eV, a relatively large width, the energy level spacing in the JDOS approaches Γ at a cluster size of 500 atoms. The range of interest for Γ could extend as much as four orders of magnitude lower, requiring clusters of millions of atoms for clear resolution of the Lorentzian.

To circumvent this limitation, it was necessary to devise another way of extracting Γ from the projected density of states. A number of statistical methods were first attempted, treating the JDOS as a set of data points to be fitted to a probability distribution. However, since these methods are often sensitive to the distribution of data points, secondary features in the JDOS frequently distorted the best-fit distribution, resulting in unreliable estimates for Γ. The time-dependent population of the adsorbate level was also examined, but no reliable method for matching the periodic population function of a finite system to the aperiodic exponential decay found in the macroscopic system could be developed.

The most reliable way to estimate Γ turned out to involve a Lorentzian broadening of the JDOS, but instead of a minimal broadening parameter, we apply a very large broadening, $\beta \gg \Gamma$. The FWHM of the resulting peak is directly related to Γ, due to an algebraic property of the Lorentzian distribution. This distribution can be represented as the fourier transform of an exponential

$$A^{\Gamma}(\epsilon - \mu) = \frac{\Gamma/2\pi}{(\epsilon - \mu)^2 + (\Gamma/2)^2} = \int e^{i\omega t} d\omega \exp\left(-it\mu - \frac{\Gamma}{2}|t| \right). \tag{4}$$

The convolution of this Lorentzian with another of width β can be rewritten using a product of fourier transforms:

$$\begin{aligned} A^{\Gamma}(\epsilon - \mu) * A^{\beta}(\epsilon) &= \int e^{i\epsilon t} dt \exp\left(-it\mu - \frac{\Gamma}{2}|t| \right) \exp\left(-\frac{\beta}{2}|t| \right) \\ &= \int e^{i\epsilon t} dt \exp\left(-it\mu - \frac{\Gamma + \beta}{2}|t| \right). \end{aligned} \tag{5}$$

This is just another Lorentzian of width $\Gamma + \beta$. Therefore, if we know the FWHM of the broadened spectrum, we can extract the original width, Γ by subtracting the broadening parameter $\Gamma = \mathrm{FWHM} - \beta$

In the present calculation, we will use a local exchange correlation potential in the density functional scheme. The local density approximation does not include the image potential of the electrons. The image potential is the dominant contribution to the energy shift of atomic levels near surfaces. For this reason, the present investigation is limited to the study of the widths of the atomic resonances. The image charges induced on metal surfaces are relatively extended, and although the barriers they introduce for electron tunneling can be significant,[4] we do not expect them to induce a strong lateral corrugation of the widths. Consequently, we expect the LDA results to well describe the lateral corrugation of the width along the surface.

Computational constraints and approximations in the model impose limits on the adsorbate-cluster configurations that can be effectively studied with the present method. When the adsorbate is extremely close to the cluster (3 a.u. or less), the resonance width approaches the scale of features in the energy spectrum of the substrate. In this case, the spectral function is distorted from a perfect Lorentzian curve, and the width of the dominant JDOS feature may be significantly different from Γ. For an accurate representation of the surface, the dimensions of the cluster must be larger than the

atom-surface separation. With current computational resources, we have had difficulties converging widths for atom-surface separations larger than 12 a.u.

III. CLUSTER SIZE EFFECTS

Another complication that must be taken into account when studying the interaction of an atom with a surface modeled using a finite cluster is quantum size effects, i.e., electronic states caused by the boundaries of the cluster. Within the intermediate range of adsorbate-cluster distances 3–10 a.u., we found quantum size effects to be the largest source of the cluster size dependence in the calculated resonance width. In this section we investigate variation of Γ with cluster size and shape. In order to be able to model very large clusters, we use the semiempirical tight binding approach in this subsection. We expect the criteria for cluster size convergence to be similar in tight-binding and density functional theory.

In the following two subsections, we investigate the effect of cluster size on the widths of the atomic levels. In the first subsection, a general result is obtained. In the second subsection, we investigate quantum size effects using clusters of different sizes and shapes.

A. Volume effects

The effect of finite cluster size can be modeled with the scattering method developed by Krueger and Pollmann.[20] The cluster boundary is treated as an infinitely high potential barrier that perturbs the semi-infinite surface. We construct an infinite array of such barriers, dividing the surface into a superlattice of clusters. The scattering method gives the resulting Green's function, projected onto any atom in the cluster:

$$G_{nn} \approx G_{nn}^{(\infty)} - \sum_{m} \frac{|G_{nm}^{(\infty)}|^2}{G_{mm}^{(\infty)}}, \tag{6}$$

where n is any atomic level and m are only those levels that fall inside the potential barrier. The superscript (∞) indicates Green's functions in the semi-infinite surface, i.e., before the potential barriers are introduced. It can be shown that the square modulus of the intersite Green's function $|G_{nm}^{(\infty)}|^2$, decays as r_{nm}^{-2} in a free electron metal. This relation is not surprising, as it is already known that the inter-site density matrix decays with the inverse square of distance in a metal.[21]

The distance to the barrier varies linearly with cluster diameter L so $|G_{nm}^{(\infty)}|^2$ is proportional to L^{-2}. However, the sum over m will include fewer atoms as the cluster size increases, since the ratio of cluster surface area to enclosed volume goes as L^{-1}. Therefore, the total sum is proportional to L^{-3}:

$$G_{nn} - G_{nn}^{(\infty)} \propto L^{-3}. \tag{7}$$

Next, we introduce the adsorbate-surface interaction. Let V_{ln} denote the Hamiltonian matrix element between adsorbate orbital Ψ_l and surface state Ψ_n. Using the Golden rule approximation, the tunneling rates between the adsorbate and the surface can be expressed in terms of the Green function

$$\Gamma \approx \sum_{n} |V_{ln}|^2 \operatorname{Im} G_{nn}. \tag{8}$$

Within the Golden Rule approximation, the volume dependence of the width therefore take the form

$$\Delta\Gamma_{\text{size}} \approx \sum_{n} |V_{ln}|^2 (\operatorname{Im} G_{nn} - \operatorname{Im} G_{nn}^{(\infty)}). \tag{9}$$

Using Eq. (7), the following expression for the volume dependence of the width is then obtained,

$$\Delta\Gamma_{\text{size}} \propto \frac{\Gamma}{L^3}. \tag{10}$$

B. Quantum-size effects

For intermediate atom-surface separation distances (3–10 a.u.), quantum size effects are the largest source of uncertainty in calculating resonance widths from finite clusters. To study these size effects, we have constructed a semiempirical tight-binding model of aluminum according to the method of Slater and Koster.[22] Tight-binding parameters developed by Krueger and Pollmann were used,[23] and the Hamiltonian eigenvalue problem was solved using the ARPACK library developed at Rice University.[24]

The tight-binding study was conducted to meet two primary goals: qualitative understanding of the size dependence of the density of states, and quantitative estimates of the cluster size necessary to calculate Γ with acceptable accuracy. We begin by discussing the qualitative part of these results.

Figure 1 shows the total density of states for cubic aluminum clusters of various sizes. In each case, the DOS follows the general form of the macroscopic distribution, but is modulated by the size quantization of energy states. For the largest clusters, the distribution of one-electron eigenstates is quite analogous to a deep, three-dimensional square well with approximately the same geometry as the cluster.

Next, we added an idealized alkali adsorbate to each cluster to simulate the interaction of a free lithium atom with its surface. The adsorbate energy levels were set to the experimental values for Li $2s$ and $2p$ orbitals.[25] To estimate aluminum-lithium coupling parameters, a single reference calculation was performed using GAUSSIAN99 with a lithium atom located 6.0 a.u. above the top site of a small aluminum cluster. The Hamiltonian matrix elements between Li$(2s)$ and Li$(2p)$ orbitals and the Al$(3s)$ and Al$(3p)$ orbitals were extracted, and used for the Al-Li tight-binding parameters.

The adsorbate is assumed to be in the top position at the center of the surface of the cluster. We only include the nearest neighbor interactions. While this model is not expected to be numerically accurate in representing the Li-surface interaction, it provides a qualitative picture of the relationship between cluster size and the adsorbate-resolved density of states (JDOS).

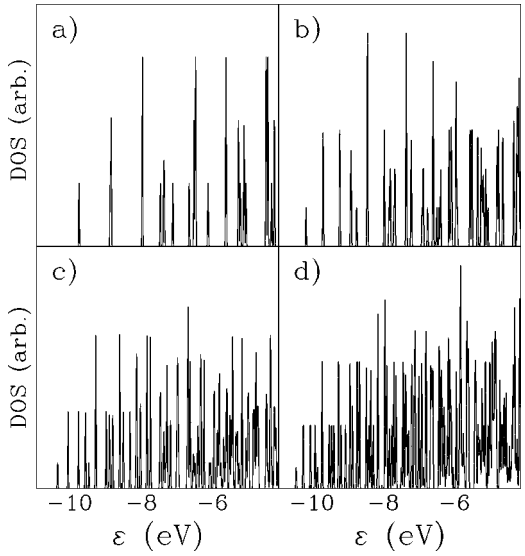

FIG. 1. Total density of states for semiempirical tight-binding models of four cubic aluminum clusters. Panel (a) refers to a cluster containing $5\times5\times5$ atoms, (b) refers to a $7\times7\times7$ cluster, (c) refers to a $9\times9\times9$ cluster, and panel (d) refers to a cluster containing $11\times11\times11$ atoms. The tight-binding parameters were taken from Ref. 23 and are $\varepsilon_{3s}=-2.421$, $\varepsilon_{3p}=6.204$, $\varepsilon_{3d}=15.176$, $V_{ss\sigma}=-0.682$, $V_{sp\sigma}=-1.163$, $V_{sd\sigma}=0.878$, $V_{pp\sigma}=2.260$, $V_{pp\pi}=-0.331$, $V_{pd\sigma}=-2.185$, $V_{pd\pi}=0.563$, $V_{dd\sigma}=-1.603$, $V_{dd\pi}=1.059$, and $V_{dd\delta}=-0.474$ eV.

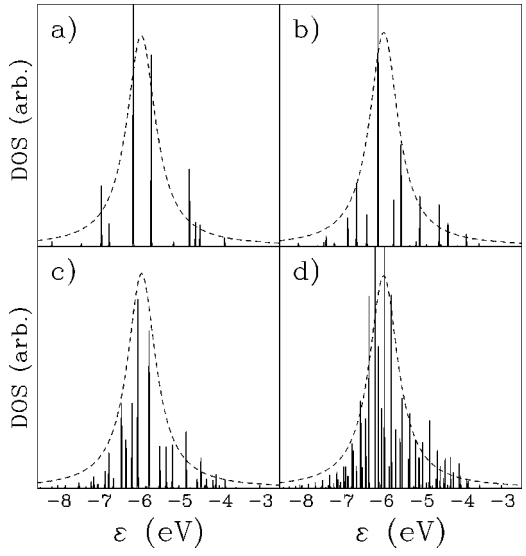

FIG. 2. The adsorbate-projected density of states (JDOS) for the Li($2s$) level on Al clusters consisting of aluminum columns of increasing depth, as calculated via a tight-binding model. Panel (a) refer to a cluster containing $6\times5\times5$ atoms, panel (b) refers to a $12\times5\times5$ cluster, panel (c) refers to a $25\times5\times5$ cluster, and panel (d) refer to a cluster containing $50\times5\times5$ atoms. The tight-binding parameters describing the Al-Al interactions are the same as in Fig. 1. To model the Li-Al interaction we use $\varepsilon_{2s}=-5.38$, $\varepsilon_{2p}=-3.53$, $V_{ss\sigma}=-1.224$, $V_{sp\sigma}=-1.713$, $V_{pp\sigma}=0.921$, and $V_{pp\pi}=-0.171$ eV. A Lorentzian with the extracted width is superimposed on the raw JDOS. The width were extracted using $\beta=2.0$ eV.

In addition to the cubic clusters described previously, two new cluster shapes were added; they included tall columnlike clusters of fixed surface area but variable depth, and flat platelike clusters of fixed depth but variable width. This revealed a key difference between cluster depth variation and cluster width variation of the JDOS.

Figure 2 shows the Li($2s$) JDOS for a series of aluminum column clusters of increasing depth. As the column depth increases, the JDOS changes in a fairly uniform manner; the eigenstates become more closely spaced, but follow the same general pattern. In the figures we also include Lorentzians with widths obtained from the calculated JDOS.

Figure 3 shows the Li($2s$) JDOS for a series of aluminum platelike clusters, each one three layers deep but of increasing lateral dimension. The JDOS of the platelike clusters changes much more unpredictably with cluster size than the columns. Even a small change in lateral cluster size can result in a very different distribution of eigenstates. Also in this figure we include Lorentzians with widths obtained from the calculated JDOS.

In Fig. 4, we show the effect of β on the width extracted from the JDOS. The calculated resonance width Γ is plotted versus the broadening parameter β for tight-binding models of two aluminum clusters. The clusters have the same lateral shape, but one is approximately twice as deep. The figure shows that the calculated Γ becomes less sensitive to β as the cluster size increases. The figure clearly shows that our procedure for extracting the level width from the JDOS is stable and relatively insensitive to β.

The difference between vertical and lateral cluster size effects can be generally understood in terms of the square

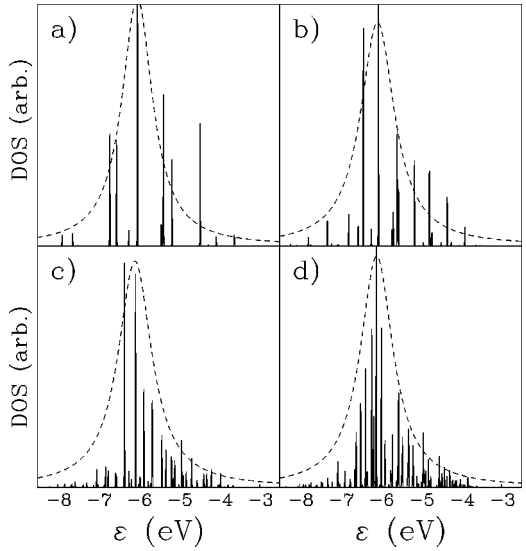

FIG. 3. The adsorbate-projected density of states (JDOS) four the Li($2s$) level on a Al clusters consisting of aluminum squares of increasing width, as calculated via a tight-binding model. Panel (a) refers to a cluster containing $7\times7\times3$ atoms, panel (b) refers to a $11\times11\times3$ cluster, panel (c) refers to a $25\times25\times3$ cluster, and panel d) refers to a cluster containing $21\times21\times3$ atoms. The tight-binding parameters are the same as those in Fig. 2. A Lorentzian with the extracted width is superimposed on the raw JDOS. The width were extracted using $\beta=1.0$ eV.

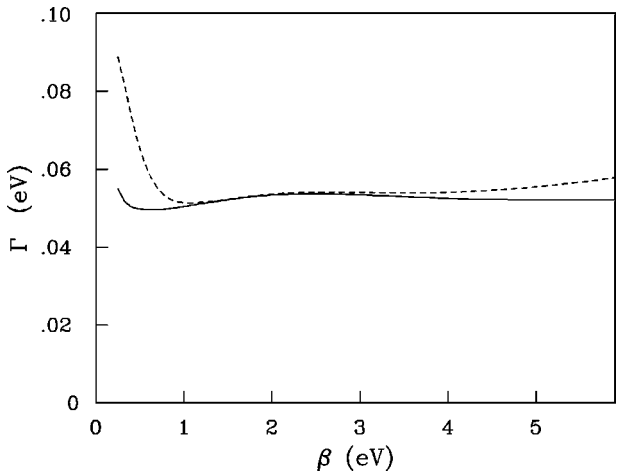

FIG. 4. The calculated resonance width Γ is plotted versus the broadening parameter β for tight-binding models of two aluminum clusters. The solid line is for a cluster containing $5\times5\times13$ atoms, and and the dashed line is for a cluster measuring $5\times5\times25$ atoms.

well model. If we match each square well eigenstate with a similar Bloch state in the cluster, its wave function will be as follows, up to a normalization constant:

$$\psi_{k\sigma}(\vec{r})=\sum_i \sin(\vec{R}_i\cdot\vec{k})\,\phi_\sigma(\vec{r}-\vec{R}_i) \tag{11}$$

with $\vec{k}=(\pi n_x/L_x)\hat{x}+(\pi n_y/L_y)\hat{y}+(\pi n_z/L_z)\hat{z}$. This wave function is written in a coordinate system where the origin lies at one corner of the cluster, therefore the cluster atom nearest the adsorbate has coordinates $(L_x/2,L_y/2,0)$. Accordingly, we can write the Hamiltonian matrix elements involving the adsorbate and a cluster eigenstates as follows:

$$H_{l\sigma,k\sigma}=\sin\left(\frac{\pi n_x}{2}+\frac{\pi n_y}{2}\right)V_\sigma,$$

$$H_{k\sigma,k\sigma}=E_\sigma+\frac{\pi^2}{2}\left(\frac{n_x^2}{L_x^2}+\frac{n_y^2}{L_y^2}+\frac{n_z^2}{L_z^2}\right), \tag{12}$$

where E_σ is an energy level of the cluster atoms, and V_σ is the matrix element between the adsorbate orbital and an orbital of the nearest cluster atom. The form of these matrix elements explain why the change of the JDOS with lateral dimension of the cluster are more irregular than the changes caused by cluster depth variation. It is as if the adsorbate is interacting with several bands, each labeled by one (n_x,n_y) pair. Within each band, the states are spaced uniformly and have the same interaction matrix element with the adsorbate. Increasing the depth of the cluster packs the eigenvalues more closely, but does not fundamentally change the shape of the band or its adsorbate interaction. On the other hand, a change in the lateral dimension of the cluster rearranges all the bands and the strength of their interactions with the adsorbate, resulting in a different JDOS.

The results of this study suggest trends in the cluster size convergence of the level width calculations. As cluster depth increases, the JDOS keeps roughly the same structure but is better resolved, therefore we would expect the calculated Γ to converge fairly smoothly toward some limit. As the lateral dimension of the cluster increases, however, the JDOS changes more unpredictably. Therefore, we expect Γ to vary somewhat randomly as the cluster width changes, making its convergence more difficult to recognize.

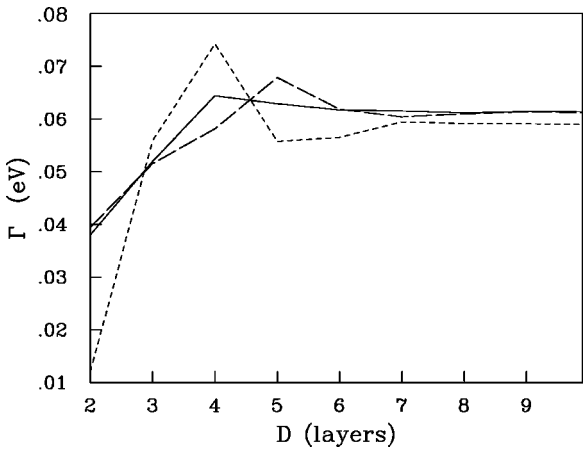

FIG. 5. Width of the Li($2s$) level as a function of cluster depth D for three clusters of different lateral dimensions. The dotted line is for a $3\times3\times D$ cluster. The dashed line is for a $5\times5\times D$ cluster and the solid line is the result for a $7\times7\times D$ cluster. The tight binding parameters are the same as those in Fig. 2. The widths were extracted using $\beta=2.0$ eV.

In Fig. 5, the resonance width Γ is plotted versus cluster depth. Each curve represents clusters with the same lateral cross section, i.e., the same L_x and L_y dimensions. Although each curve converges clearly toward a limiting value of Γ, it would be misleading to conclude that any one of these is the semi-infinite limit. Each lateral cross section produces a different large-depth limit for Γ, and these limits will only agree when the lateral dimensions of the cluster are large.

The second goal of the tight-binding study is to estimate the cluster size necessary to accurately determine Γ. First of all, a cluster depth must be chosen. In all the depth versus Γ plots shown above, Γ rises up to a critical depth, then rapidly decays to its large-depth limit. At five layers deep, all clusters are past their critical depth and Γ is within approximately 10% of its limit. At six layers, Γ is within 2% of its large-depth limit, regardless of lateral dimensions.

Once a cluster depth is selected, the lateral dimensions must be chosen. From the clusters studied, it appears that the smaller of the two lateral dimensions determines the accuracy of Γ. In Fig. 6, Γ is plotted versus the minimum lateral dimension of each cluster. Five-layer deep clusters are within 10% of the macroscopic Γ, even for very small lateral dimensions. Increasing their lateral size beyond three or four atomic planes will gain little accuracy in Γ. Six-layer deep clusters should be somewhat wider; clusters about five atomic planes wide are necessary before the uncertainty in Γ is 2% or less.

IV. RESULTS

The method for determining adsorbate level widths described in the previous section is now applied to two physi-

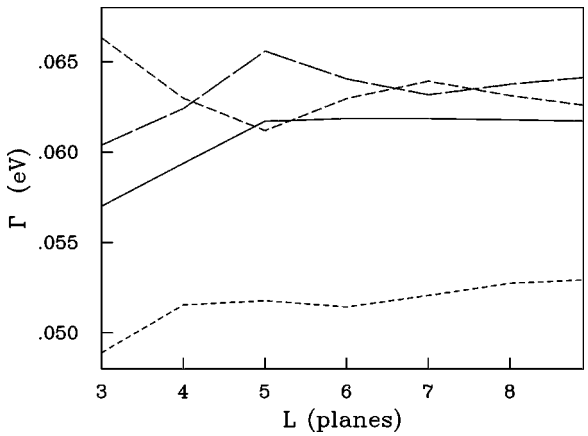

FIG. 6. Width of the Li(2*s*) level versus the shortest lateral cluster dimension *L*, for four clusters of different depths. The dotted line refers to a $L\times11\times3$ cluster, the short-dashed line refers to a $L\times11\times4$ cluster, the long-dashed line is for a $L\times11\times5$ cluster and the solid line is the result obtained for a $L\times11\times6$ atom cluster. The tight-binding parameters are the same as those in Fig. 2. models of aluminum. Clusters five and six layers deep were studied. The widths were extracted using $\beta=2.0$ eV.

cal systems: Li(2*s*)/Al(001) and Li(2*s*)/Si(110). In both cases, the density functional method was used to determine the ground state electronic structure of the adsorbate-cluster system, and the calculation of the projected density of states.

A. Density functional method

The density functional method provides a much more physically accurate calculation of electronic structure than our tight-binding model. It is an *ab initio* method, requiring no semiempirical parameters, and it includes charge redistribution and correlation effects. The disadvantage is its computational cost, so that cluster sizes must be smaller than in the tight-binding study.

The first step in determining resonance widths is to find the ground state electronic structure of the adsorbate-cluster system. For this purpose we used CMOL,[26] an electronic structure code previously developed at Rice. CMOL uses the density functional formalism under the local spin density approximation, so both charge self-consistency and some correlation effects are taken into account.

In each calculation, the surface is represented by a cluster of the same chemical composition as the substrate. These clusters are not relaxed, but instead fixed in the bulk geometry of the cluster. While a relaxed cluster would be more physical in isolation, it may be less similar to the macroscopic surface. The primary disadvantage of unrelaxed clusters is the slow convergence of the electronic structure; however, in the systems we studied the convergence was sufficiently fast for our needs.

An important goal of the present work is to enable the calculation of resonance widths for arbitrary adsorbate positions. Therefore, restricting the atom-cluster configuration to high symmetry positions is undesirable. However, it is possible to take advantage of symmetry in the surface normal direction without restricting the adsorbate position. For each system in the present study, all atoms were reflected across the crystal plane farthest from the adsorbate. This generates a cluster approximately twice as large with two identical adsorbate atoms on opposite faces, but with very little increase in computational cost. Interactions between the two adsorbates are very small due to their large separation distance, and due to the screening induced by the cluster. It is also possible to take advantage of lateral symmetry, and still explore adsorbate positions over a large portion of the surface unit cell.

B. Li on Al(001)

The surface is modeled using five different cluster geometries shown in Fig. 7. The figure also shows the planes or lines of symmetry along which the adsorbate is placed. The first two clusters are three layers deep and five layers wide along their shortest lateral dimension. These broad, shallow clusters are designed to allow adsorbate positioning any-

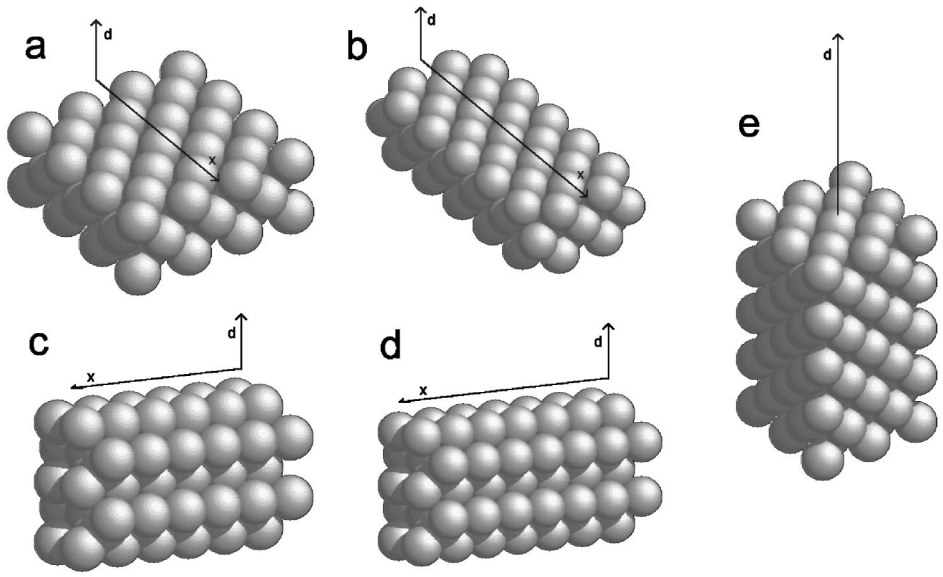

FIG. 7. Aluminum clusters used in the density function study of lithium on the Al(001) surface.

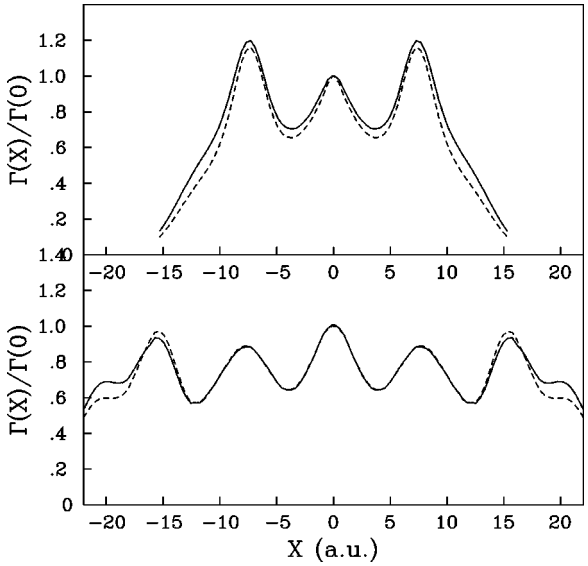

FIG. 8. Width of the Li($2s$) level as a function of lateral position over Al(001), including top and center sites. The upper panel shows the results for cluster a and the lower panel are the results for cluster b. The dotted lines shows the level widths obtained using $\beta=1$ and the solid lines were obtained using $\beta=2$ eV. The adsorbate is separated from the surface by 8.5 a.u. The top site at the center of the upper face of the cluster is chosen as the origin $X=0$.

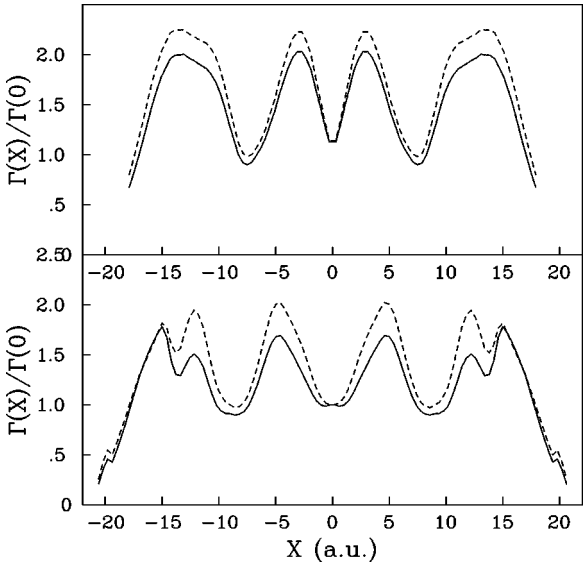

FIG. 9. Width of the Li($2s$) level as a function of lateral position over Al(001), including center and bridge sites. The upper panel are the results from cluster c and the lower panel are the results for cluster d. The dotted lines shows the level widths obtained using $\beta=1$ and the solid lines were obtained using $\beta=2$ eV. The adsorbate is separated from the surface by 8.5 a.u. A center site on the center of the upper face of the cluster is chosen as the origin $X=0$.

where along the longest lateral axis while keeping fourfold symmetry to reduce computational cost. The second and third clusters have similar size to the first two, but their lateral axes are rotated 45° from the crystal axes. These clusters are also designed to allow lateral adsorbate movement, but along a different direction than the first two.

The Γ values obtained from these clusters are somewhat sensitive to the broadening parameter β with which Γ is extracted. Since the focus of the present work is to investigate the lateral variation of the adsorbate level width, Γ is rescaled so that its value at the center of the trajectory is unity.

Figure 8 shows the variation of the rescaled Γ as the lithium adsorbate moves along a trajectory that passes over the center and top sites, i.e., in the (100) direction. After the rescaling, the corrugation of Γ is relatively insensitive to cluster size, especially in the central part of each cluster surface. One would therefore expect that the corrugation of Γ calculated for these clusters accurately reflects the corrugation expected on an infinite surface.

Figure 9 shows the lateral dependence of Γ along a trajectory that passes over the center and bridge sites, i.e., in the (110) direction. Again, Γ is rescaled to equal one at the center site, and after rescaling it is nearly independent of cluster size.

In Fig. 10, the dependence of the width on adsorbate-substrate separation is shown. The Li atom is placed on the top site of the cluster (e). This large cluster measures nine layers deep and five layers wide in both lateral dimensions. This cluster is designed for a more restricted range of adsorbate positions along the vertical axis, where the system has eightfold symmetry. The Γ values calculated from this cluster are expected to be fairly accurate, as the cluster is well within the size guidelines developed from the tight-binding study. The two solid curves in Fig. 10 were obtained with different broadening parameters, 1.0 and 2.0 eV, showing that the results are relatively insensitive to β. At adsorbate-

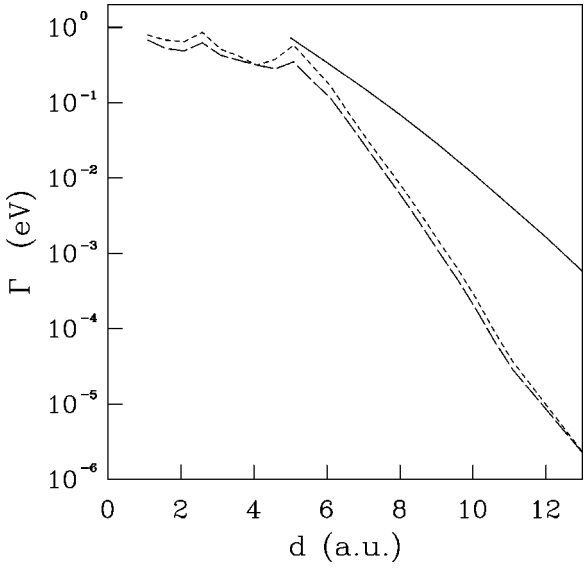

FIG. 10. Width of the lithium ($2s$) level versus vertical distance above the Al(001) top site on cluster *e*. The dotted line shows the widths calculated using $\beta=1$ and the dashed lines are widths obtained using $\beta=2$ eV. The solid line shows the results from complex scaling theory (Ref. 4).

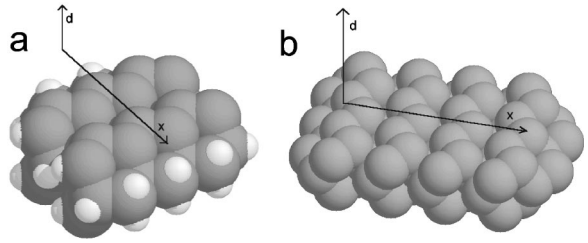

FIG. 11. Silicon clusters used in the density functional study of lithium on the Si(110) surface.

cluster distances greater than about 8 a.u., the tunneling rate calculated from these results is not reliable. In this range, the separation distance approaches the length scale of the cluster diameter, and the electronic wave functions of the cluster decay much faster than the wave functions from a macroscopic surface. Figure 10 also includes the results obtained by the complex scaling method for a lithium adsorbate on a jellium surface modeling Al.[4] The cluster data clearly follows the latter pattern, indicating that cluster size effects are primarily caused by changes in the cluster wavefunctions near the adsorbate. The present LDA widths are smaller than the complex scaling results. One contributing factor to this difference is that the LDA results neglect the image potential which lowers the tunneling barriers between the atom and the surface.[4]

The calculation show a large lateral corrugation of the width of the Li($2s$) level outside Al(001). The width directly above an Al atom is a factor of two smaller than when the Li atoms is above a hollow position.

C. Li on Si(110)

Charge transfer between an adsorbate and a semiconducting surface is not as well understood as for a metal surface. In a semiconductor, the density of states is very different from a free-electron metal, and the electron eigenstates can be more localized. Both of these factors make it difficult to apply the conventional analytic theories for resonance energy calculations to semiconducting or insulating surfaces.

Two cluster models were used to simulate a lithium atom on the silicon (110) surface. As with the aluminum study, the clusters were not relaxed so that they would more accurately represent the macroscopic surface. To speed convergence of electronic structure calculations, the dangling silicon bonds along the sides of the smaller clusters were terminated with hydrogen. The top and bottom faces, where the adsorbates interact, were left clean. The geometry of these silicon clusters is shown in Fig. 11.

Both clusters have the same depth, but one has larger lateral dimensions to test cluster size convergence of the results. In both cases, the lithium adsorbate was positioned in a plane parallel to the surface normal vector, and parallel to the longest lateral dimension of the cluster. The resulting system had four-fold symmetry regardless of adsorbate position in that plane.

In Fig. 12, the widths of the Li(2s) level are shown along a trajectory in the (001) direction, which runs perpendicular to the ridges and troughs characteristic of the (110) silicon

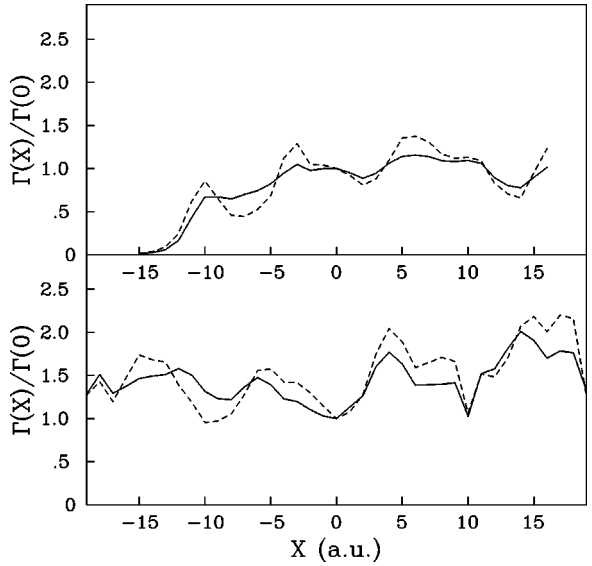

FIG. 12. $L(2s)$ level broadening versus lateral position over Si(110). The upper panel are the results obtained using cluster a and the lower panel are the results using cluster b. The dotted line shows the widths calculated using $\beta=1$ and the dashed lines are widths obtained using $\beta=2$ eV. The origin ($X=0$) is located directly above an atom in the second Si layer.

surface. For each cluster, only the innermost unit cell was selected for calculation of Γ to minimize edge effects. As with the aluminum study, Γ is rescaled, in this case so that it is unity at its maximum, and widths are extracted with broadenings of both 1.0 and 2.0 eV.

The lateral variation of Γ shows stronger, less sinusoidal variation than for the aluminum clusters. This is expected because the screening of the atom surface interaction is less efficient on a semiconductor surface than on a metal. The corrugation of the electron potential is deeper, and has a longer length scale than on an aluminum surface. However, it may also result from greater localization of electron eigenstates. As the adsorbate encounters these localized states, the matrix elements between adsorbate and surface wave functions increase exponentially, resulting in an increased tunneling rate.

The corrugation of the the Li($2s$) width on the Si surface is also more sensitive to the broadening parameter β with which it is extracted than what was the case for Li on Al. This may simply be due to the small cluster size used in this study, but it is also possible that the spectral function is more non-Lorentzian due to the pronounced energy dependence of the DOS arising from the band structure of silicon. For a non-Lorentzian JDOS, the method for extracting widths from the JDOS should be modified.

V. CONCLUSIONS AND OUTLOOK

In this work, we have demonstrated a new method for calculating the electron tunneling rate between a surface and an incident, low-energy adsorbate. The surface is represented by a finite cluster reflecting the composition and lattice structure of the macroscopic substrate. To find the tunneling rate,

the electronic structure of the adsorbate-cluster system is calculated numerically, and the density of states is projected on chosen adsorbate orbitals. This projected density of states is then convoluted with a broad Lorentzian distribution, and the resulting full width at half-maximum of the result is extracted.

With present computational resources, the most significant limitation of the method is the restricted range of separation distance between the adsorbate and the cluster interface. When this distance approaches the length scale of the cluster, the cluster wave functions begin to decay much faster than for a semi-infinite surface. This distorts the Hamiltonian matrix elements and results in inaccurate widths.

The present calculation utilized the local density approximation for the calculation of the electronic structure of the adsorbate/surface system. This approach was taken for computational simplicity and would not be the ideal method for a quantitative calculation of adsorbate resonance energies. The LDA suffers from a range of unphysical characteristics, such as the neglect of van der Waals forces, image forces, and the lack of the property of integer preference. We do not expect that any of these properties will influence the magnitude of the lateral corrugation of adsorbate levels which is a property primarily determined by the variation of the local hybridization between the adsorbate levels and the substrate levels. However, an accurate determination of both the absolute magnitude of the tunneling rates and the shift of the adsorbate levels will require an electronic structure method that does not suffer from some of the unphysical deficiencies of LDA. In addition, for the calculation of the adsorbate level shifts and interaction potential, one must correct for the basis set superpositions errors expected for large adsorbate-surface separations. The state of electronic structure calculation methodology is a rapidly evolving field and once more accurate methods such as nonlocal or time-dependent density functional theory[27] or hybrid density functional/CI schemes[28] are available, they should be used. With such approaches, both the energy shifts and widths as well as the interaction potential between the adsorbate and the surface could in principle be obtained within a single calculation.

The method present here can be applied to atoms and molecules interacting with surfaces of arbitrary geometry and composition, including semiconductors, insulators and heterogeneous systems. The accuracy of the results is limited only by computational resources, and even the separation distance limit can be increased by employing larger clusters.

This work was supported by the Robert A. Welch foundation.

*Corresponding author. Fax: (713)348-4150; e-mail: nordland@rice.edu

[1] J. Los and J. J. C. Geerlings, Phys. Rep. **190**, 133 (1990).
[2] B. H. Cooper and E. R. Behringer, in *Low Energy Ion-Surface Interactions*, edited by J. W. Rabalais (Wiley, New York, 1994), pp. 263–312.
[3] J. P. Gauyacq and A. G. Borisov, J. Phys.: Condens. Matter **10**, 6585 (1998).
[4] P. Nordlander and J. C. Tully, Phys. Rev. B **42**, 5564 (1990).
[5] D. Teillet-Billy and J. P. Gauyacq, Surf. Sci. **239**, 343 (1990).
[6] P. Kurpick and U. Thumm, Phys. Rev. A **58**, 2174 (1998).
[7] S. A. Deutcher, X. Yang, and J. Burgdorfer, Phys. Rev. A **55**, 466 (1997).
[8] V. Ermoshin and A. K. Kazansky, Phys. Lett. A **218**, 99 (1996).
[9] G. A. Kimmel and B. H. Cooper, Phys. Rev. B **48**, 12 164 (1993).
[10] S. B. Hill, C. B. Haich, Z. Zhou, P. Nordlander, and F. B. Dunning, Phys. Rev. Lett. **85**, 5444 (2000).
[11] C. C. Hsu, H. Bu, A. Bousetta, J. W. Rabalais, and P. Nordlander, Phys. Rev. Lett. **69**, 188 (1992).
[12] L. Houssiau, J. W. Rabalais, J. Wolfgang, and P. Nordlander, Phys. Rev. Lett. **81**, 5153 (1998).
[13] I. Vaquila, K. M. Lui, J. W. Rabalais, J. Wolfgang, and P. Nordlander, Surf. Sci. **470**, 255 (2001).
[14] P. Nordlander and N. D. Lang, Phys. Rev. B **44**, 13 681 (1991).
[15] J. A. M. C. Silva, J. Wolfgang, A. G. Borisov, J. P. Gauyacq, P. Nordlander, and D. Teillet-Billy, Nucl. Instrum. Methods Phys. Res. B **157**, 55 (1999).
[16] A. G. Borisov, A. K. Kazansky, and J. P. Gauyacq, Phys. Rev. B **59**, 10 935 (1999).
[17] J. Merino, N. Lorente, P. Pou, and F. Flores, Phys. Rev. B **54**, 10 959 (1996).
[18] T. Klamroth and P. Saalfrank, Surf. Sci. **410**, 21 (1998).
[19] S. W. Gao and D. S. Wang, J. Phys.: Condens. Matter **2**, 2187 (1990).
[20] P. Kruger and J. Pollmann, Phys. Rev. B **38**, 10 578 (1988).
[21] S. Goedecker, Phys. Rev. B **58**, 3501 (1998).
[22] J. C. Slater and G. F. Koster, Phys. Rev. **94**, 1498 (1954).
[23] K. Wuerde, A. Mazur, and J. Pollmann, Phys. Status Solidi B **179**, 399 (1993).
[24] D. Sorensen (private communication).
[25] W. C. Martin and W. L. Wiese, in *Atomic, Molecular and Optical Physics Handbook*, edited by G. W. F. Drake (AIP, Woodbury, NY, 1996), Chap. 10, pp. 135–153.
[26] L. Lou and P. Nordlander, Phys. Rev. B **54**, 16 659 (1996).
[27] *Electronic Density Functional Theory: Recent Progress and New Directions*, edited by J. F. Dobson, G. Vignale, and M. P. Das (Plenum Press, New York, 1998).
[28] N. Govind, Y. A. Wang, and E. A. Carter, J. Chem. Phys. **110**, 7677 (1999).